Quantifying Velocity, Chlorophyll, Temperature, and Nutrients Relationships with Primary Productivity in the Western Equatorial Pacific

Emma Nguyen

University of Washington, Seattle, WA

School of Oceanography

Email: emman23@uw.edu

March 8, 2024

Abstract

Net primary productivity (NPP) and gross primary productivity (GPP) is a major component of the carbon cycle. NPP is defined as the amount of carbon biomass produced by primary producers over a given period of time and area. GPP is the combination of NPP and respiration. The NPP exceeds 100 billion tons of carbon per year on Earth and half of it comes from the ocean through phytoplankton. The equatorial Pacific Ocean is the largest tropical ocean on Earth and subsequently the largest oceanic source of CO2 to the atmosphere. Despite its importance, NPP in the west equatorial Pacific is poorly characterized due to the lack of data. Previous research suggests that strong upwelling is associated with increased nutrient concentration in the euphotic zone leading to an increase in primary productivity. However, the western equatorial Pacific is known for weaker upwellings compared to the eastern and central equatorial Pacific. This study was conducted aboard the R/V Thomas G. Thompson from December 28, 2023, to January 12, 2024, with the goal of identifying and quantifying the critical variables that have a substantial impact on NPP in the region including temperature, chlorophyll, dissolved nutrients, and current velocity. NPP and GPP was measured using in-situ oxygen incubations. The mean GPP found in this study range from −163.82 to 26.05 mmol O_2 m^{-2} d^{-1}. A combination of temperature, chlorophyll, dissolved nutrients, and current velocity can explain for 54.18% of the variance in GPP. There is a missing 45.82% not accounted for that requires further studies on factors that influence GPP such as iron, which is a limiting nutrient.

Plain Language Summary

Net primary productivity (NPP) is the rate that plants and primary producers store energy and make it available for higher trophic levels. The rate is defined by the difference between the amount of carbon produced through photosynthesis and the amount of energy used by respiration. Understanding what affects the NPP rate is important for predicting climate change. This study focuses on the western equatorial Pacific, where there are weaker upwellings which in turns means it has a lower NPP rate, compared to other regions. However, there is limited research done in this region. Using the data collected from a cruise in western equatorial in the winter of 2023 and 2024, the NPP rates and driving factors such as, current velocity, nutrients, temperature, and chlorophyll were analyzed to find a correlation. There was no linear relationship found between NPP rates and the current velocity, nutrients, temperature, and chlorophyll. However, the combination of the driving factors can explain 54.18% of the GPP values. The missing 45.82% requires further research in other factors that could affect the GPP such as, iron concentration, which is the limiting nutrient in the region.

Introduction

Ocean primary productivity is the production of organic matter by phytoplankton in the ocean, a process accounting for almost half of the global net primary productivity (NPP) (Field et al., 1998). NPP is the rate of organic carbon produced by autotrophs minus the autotrophs' respiration rate (Sigman & Hain, 2012). A portion of the carbon fixed through NPP in the surface ocean sinks to the deep ocean, leading to an

accumulation of carbon. NPP can exhibit year-to-year variations influenced by factors such as nutrients, light, and temperature (Krumhardt et al., 2020). The exact influence of each factor to NPP is not clear and there may be other factors that also impacts such as the salinity of the water. Understanding the factors that impact NPP is crucial for maintaining ecosystem diversity (Sigman & Hain, 2012), marine biology (Moore et al., 2018), and fishery industries (Stock et al., 2017).

Phytoplankton are an essential energy source for marine fish populations. Based on data from 1990-1999, the global NPP will decrease which will lead to the biomass of zooplankton and phytoplankton decreasing (Lotze et al., 2019). However, human activities such as fishing, contribute to the higher trophic levels decreasing faster compared lower trophic levels in relation to NPP level. Knowing the NPP levels allows fishery industries to regulate the catches, so fisheries do not put a strain on the lower trophic level productivity. Fishing is not directly impacting NPP, but the NPP can be a control factor of how much fish is available.

NPP in the ocean is the highest near the equator and decreases toward the pole (Huston & Wolverton, 2009). The global NPP in the ocean is estimated to be 45 - 50 Pg C y^{-1} (Longhurst et al., 1995).NPP levels are highest in the epipelagic zone, which is the uppermost zone of the ocean that receives the most sunlight, and in areas near the coastline and estuaries, which are rich in nutrients. The NPP is higher at the equator than higher latitudes due to warmer temperatures and higher solar radiation which allows photosynthesis to occur year-round.

Satellites can measure the color of the surface ocean to track the concentration of green pigment chlorophyll, which is used to process light via photosynthesis.

However, the chlorophyll concentration is a better indicator the rate of photosynthesis since it is based on the rate of photosynthesis so it is a proxy for the NPP rate (Sigman & Hain, 2012). Chlorophyll concentration is one of the factors that can be used to infer NPP. Various factors, such as nitrate concentration, phosphate concentration, temperature, and mixed layer depth can influence the NPP. Phytoplankton that have adapted to lower light with high nutrient concentrations tend to have higher cellular concentration of chlorophyll (Sigman & Hain, 2012). The NPP is representative of the growth of phytoplankton biomass and the transfer of organic matter-energy to higher trophic levels (Tagliabue et al., 2021). For example, the Southern Ocean has the highest chlorophyll concentration due to the upwellings of nutrient-rich deep water and high availability of sunlight (Venables & Moore, 2010). However, the Southern Ocean does not have the highest NPP rate due to photosynthesis being limited by iron concentration (Feng et al., 2022). Due to this distinction, the satellite-derived NPP may be overestimated or underestimated in certain areas.

NPP is estimated from satellite-observations by looking at chlorophyll concentrations and various factors depending on the model. The carbon, absorption, and fluorescence-resolving (CAFE) model calculates the NPP as the product of the energy absorption, and the efficiency by which absorbed energy is converted into carbon biomass (Silsbe et al., 2016). The energy absorption is calculated from the concentration of chlorophyll-a and the size of the phytoplankton cells (Silsbe et al., 2016). Eppley-VGPM is a hybrid version of vertically generalized production model (VGPM) that assumes higher surface temperature favors high-light acclimated phytoplankton, which requires less chlorophyll to support (Behrenfeld & Falkowski,

1997). Each model accounts for different scenarios, where chlorophyll concentration or higher temperature is more important.

The equatorial Pacific is the largest tropical ocean on Earth with one of the highest NPP rates. The equatorial Pacific Ocean is also the largest oceanic source of CO_2 to the atmosphere and accounts for 20% of global productivity (Stanley et al., 2010). The equatorial Pacific is known as an area with high-nutrient and low-chlorophyll where biological utilization of nitrate and phosphate is limited by the availability of iron (Winckler et al., 2016). Previous studies suggest the upwelling of water from the Equatorial Undercurrent is a greater source for dissolved iron than dust, and therefore has a greater impact on regulating NPP in the equatorial Pacific (Winckler et al., 2016). Upwelling is the process in which cold nutrient-rich water from the deep ocean rises to the surface. The upward movement of water transports crucial nutrients, such as nitrogen and phosphorus, into the euphotic zone, supporting photosynthetic organisms (Sigman & Hain, 2012). Regions of upwelling can be determined from the distribution of sea surface temperature, where colder water is surrounded by warm water. For example, the equatorial Pacific Ocean shows an area upwelling with a thin horizontal area of lower temperatures surrounded by warmer water off the coast of South America, the chlorophyll concentration is also higher in the same area and thereby NPP, are also higher in this area.

Equatorial upwelling, with a velocity of $10^{-2}\ cm\ s^{-1}$, is more intense than mid-ocean upwelling, with a velocity of $10^{-4}\ cm\ s^{-1}$, and can be identified by temperature and density profiles (Hidaka, 1972). Wind stress curls, the thermocline, and the equatorial ocean currents are the primary drivers of the mid-ocean upwelling (Hidaka,

1972). Wind stress are the force exerted by the wind in the surface of the water and curl wind stress is the rotation of the wind stress. The thermocline is the transition layer between mixed warmer layer on the surface water and deep cooler water below. The upwelling in the eastern and central equatorial Pacific is promoted by easterly winds and pseudo-wind stress of 30-40 $m^2\,s^{-2}$ while the western equatorial Pacific wind direction is variable and the pseudo-wind stress is 10-20 $m^2\,s^{-2}$ (Mackey et al., 1995). Pseudo-wind stress is the product of the wind vector and wind stress with reference to a height above the surface. Comparing the pseudo-wind stresses, the upwelling in the western equatorial Pacific is much weaker compared to the eastern and central equatorial Pacific.

The equatorial upwelling is highly sensitive to the variation of trade winds. Strong westerlies in the western equatorial Pacific reduce upwelling, leading to uniform water temperature from the surface to the thermocline (Hidaka, 1972). In contrast, the Eastern and Central equatorial Pacific experience a higher primary productivity rate due to easterly wind and strong pseudo-wind stress (Mackey et al., 1995). The weak subsurface upwelling system in the western equatorial Pacific can be due to a layer of low-salinity warm water (Mackey et al., 1995). The salinity is lower at the equator due to frequent rainfall, which dilutes the salt content of the water. The warm temperature is due to the equatorial region having consistently high temperatures as a result of direct sunlight. The warmer, lighter surface water will not sink as deep as denser cold water. Due to the large vertical salinity changes between the surface low-salinity water and high-salinity water, the upwelling rate will decrease. The warm temperature and rainfall

stratified the upper water and reduced the nutrient input to the photic zone via upwelling resulting in a decline in NPP.

The strength of the equatorial upwelling is strongly linked to nutrient concentrations and primary productivity. The eastern and central equatorial Pacific experienced strong upwelling and are regions with high-nitrate and low-chlorophyll where production is limited by iron (Coale et al., 1996; Stanley et al., 2010). There have been few measurements of the biological activity in the western equatorial Pacific compared to the eastern and central equatorial Pacific (Behrenfeld et al., 2006; Stanley et al., 2010). The productivity in the western equatorial Pacific is estimated to be negligible to 36% of the productivity in the eastern equatorial Pacific (Stanley et al., 2010). Based on a previous study done in situ, the net community production (NCP) in the western equatorial Pacific is about 1.5 ± 0.2 mol C m^{-2} yr^{-1} (Stanley et al., 2010). NCP is the difference between NPP and total respiration (Wang et al., 2023). Currently, there are only a few published studies on the NPP in the western equatorial Pacific with most of them being estimates based on satellite-derived NPP. Based on satellite-derived NPP, the average NPP in the western equatorial Pacific is around 150-200 g C m^{-2} y^{-1}. However, satellite-derived NPP may be overestimated or underestimated due assumptions in the calculations where a factor is more important. This study aims to fill this gap by providing a detailed characterization of biological productivity in this region during December and January.

Methods

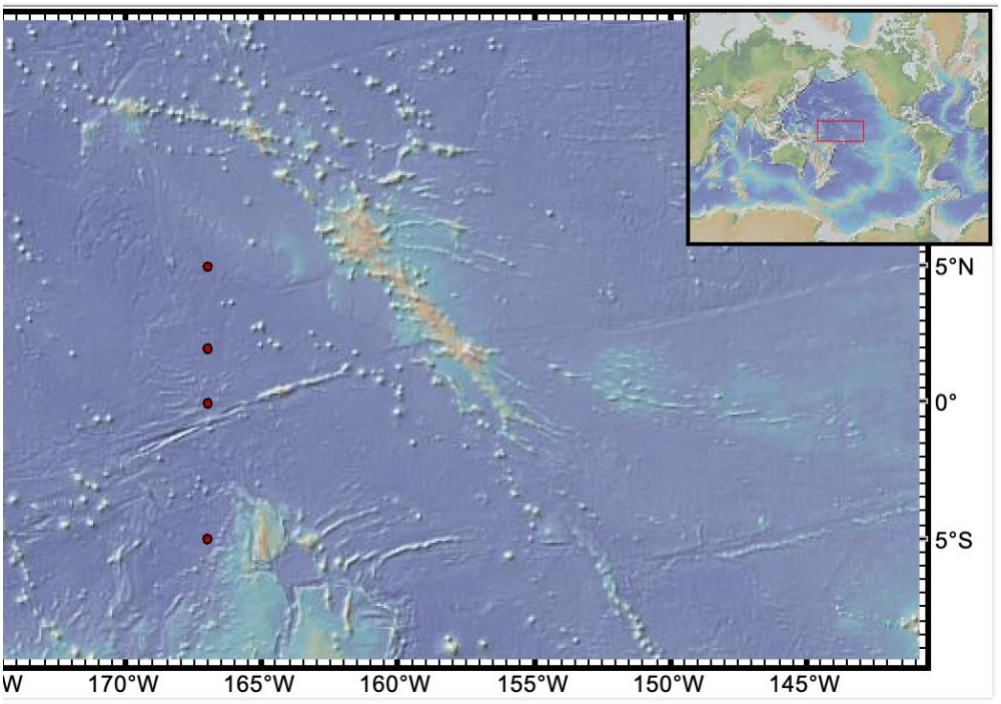

Figure 1. Map of Sample Sites at 167W; each red dots are the stations; from South to North: 5S, equator, 2N, and 5N.

This study took place from December 28, 2023, to January 11, 2024, aboard the R/V Thomas G. Thompson in American Samoa (Figure 1). Instruments on the cruise used in this study were the Sea-Bird SBE 9+ Conductivity Temperature Depth (CTD) Profiler with Niskin bottles, WetLabs ECO Fluorometer, Sea-Bird SBE 43 as the dissolved oxygen sensor, and the Teledyne RD Instruments Acoustic Doppler Current Profiler (ADCP). At the first station, 5°S, the Fluorometer was calibrated for the chlorophyll concentration and Sea-Bird SBE 43 was calibrated for the dissolved oxygen. The CTD was cast at four stations (5°S, equator, 2°N, and 5°N), starting from the southernmost station to the northernmost station (Figure 1). These four stations were chosen because the current velocity of each station vary the most from each other,

giving me the biggest range of velocity while so giving a wide spatial area for temperature, chlorophyll, and nutrients.

Oxygen Titrations based Gross Photosynthesis

Water samples of 10 liter were taken at two different depths, the mixed layer depth, about 30m, and the euphotic zone, about 60m (Stanley et al., 2010). By doing so I can measure if NPP changes with respect to depth through the mixed layer and euphotic zone. The euphotic zone determines the amount of light available to the phytoplankton and is used in the CAFE model NPP calculation (Silsbe et al., 2016). The water samples collection was the first to be sampled from the CTD due to the risk of gas

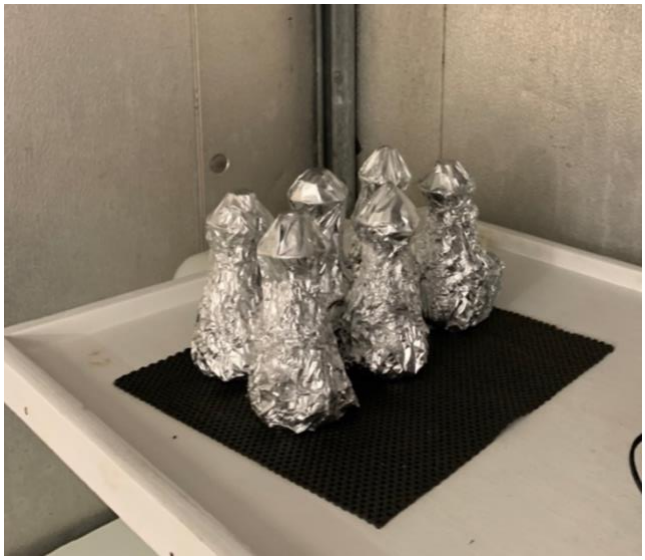

Figure 2. Dark bottles wrapped in aluminum foil in the in-situ incubation.

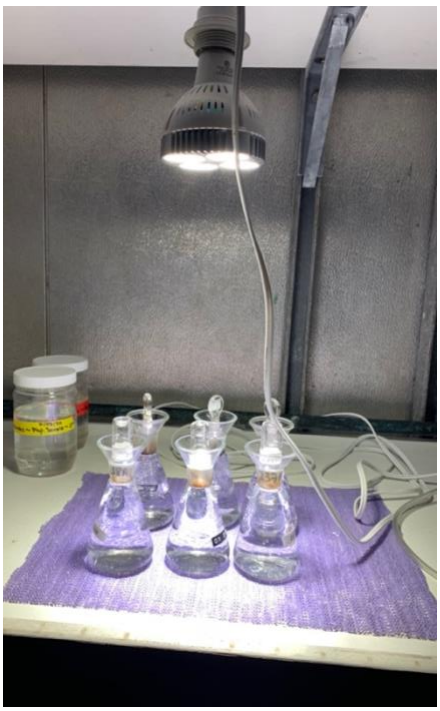

Figure 3. Light bottles in the in-situ incubation room with light shining on them for the whole incubation time.

mixing during collection. The mixed layer depth at the western equatorial Pacific is on average 29 meters (Lukas & Lindstrom, 1991). The water samples were stored in seven glass bottles of the same size with three being covered with aluminum foil to make it opaque to follow the light-dark bottle method (Mountford, 1969). Then, three clear bottles and three opaque bottles are put in an in-situ incubator for 24 hours (Figure 2 and 3). The dissolved oxygen of the initial glass bottle is measured by using the Winkler method for the initial dissolved oxygen (Labasque et al., 2004). The Winkler method is a method of measuring dissolved oxygen by adding manganese chloride and alkaline-iodide to the sample, forming an acid solution (Labasque et al., 2004). Sulfuric acid is added to react with the dissolved oxygen and potassium iodine is added to separate the iodine (Labasque et al., 2004). Then starch is added as an indicator and titrated via sodium thiosulfate until the solution turns clear (Labasque et al., 2004). After 24 hours, the dissolved oxygen of the incubated bottles is measured titrating according to the Winkler method. The titrated measurement for each bottle were used to calculate the oxygen concentration based on the Winkler method. The net oxygen production is the final dissolved oxygen in the light bottle subtracted from the initial dissolved oxygen (equation 1a). The oxygen consumed by respiration is the final dissolved oxygen in the dark bottle subtracted from the initial dissolved oxygen (equation 1b). The total oxygen produced is the oxygen consumed in the dark bottle and the oxygen produced in the light bottle (equation 1c). The total oxygen produced can be converted into the total carbon product by the Redfield ratio, 0.375 milligram carbon over milligram oxygen (equation 1d). Then, the carbon production rate is from the total carbon product divided by the incubation time (equation 1e and 1f). The dissolved oxygen production was

replicated three times for each depth for accuracy in triplicate bottles. The mean of the rates was calculated for each latitude at 30 meters and 60 meters. Photosynthesis is also referred to primary productivity. The dissolved oxygen concentration measured by the Sea-Bird SBE 43 was used to compare the initial oxygen concentration.

$$Net\ photosynthesis = Light\ Bottle\ Concentration - Initial\ Bottle\ Concentration \quad (1a)$$

$$Respiration = Dark\ Bottle\ Concentration - Initial\ Bottle\ Concentration \quad (1b)$$

$$Gross\ Photosynthesis = Net\ Photosynthesis + Respiration \quad (1c)$$

$$C{:}\,N{:}\,P{:}\,O2 = 106{:}\,16{:}\,1{:}\,138 \quad (1d)$$

$$Respiration\ Rate = \frac{Respiration}{Incubation\ Time} \quad (1e)$$

$$Net\ Photosynthesis\ Rate = \frac{Net\ photosynthesis}{Incubation\ Time} \quad (1f)$$

$$Gross\ Photosynthesis\ Rate = \frac{Gross\ Photosynthesis}{Incubation\ Time} \quad (1g)$$

Instruments Data Collection

The ADCP measures the velocity of the horizontal current, which can be compared for information if there is upwelling (Villacieros-Robineau et al., 2021). Information about the presence of upwelling can be determined by looking at the water masses movement based on the salinity and temperature data from the CTD, where the surface water temperature is cooler than the surrounding water (Fine et al., 1994). The ADCP data was post-processed by Cody Cruz using UHDAS+CODAS software from the University of Hawaii (Firing et al., 2012). In addition to removing all periods beyond 5º S and 5º N to obtain a pure transect, threshold editing was applied to eliminate velocity values in bin ensembles with less than 80% good pings or greater than 500 mm/s error velocity magnitude. The horizontal velocities were analyzed with the cross-section area of flow to determine transport in each direction.

The WetLabs ECO Fluorometer measures the fluorescence of chlorophyll-a which correlates to the NPP since there is a strong positive correlation between the increase in chlorophyll and to increase in NPP (D'Alelio et al., 2020). The fluorescence was measured from the Fluorometer in units of Relative Fluorescence Unit (RFU) and represent the chlorophyll concentration in the water at the depth. The Fluorometer took measurement at 30m and 60m for each latitude, exactly where the water samples were collected in the Niskin bottles.

The CTD profiles were used to collect the temperature of water samples. The temperature of the water samples is used to compared to the GPP. The data was analysis in the Excel to determine the mixed layer for the nutrient concentration.

The nutrients were calculated from water samples taken from 5S, equator, 2N, and 5N. The nutrient samples were sent to the University of Washington Marine Chemistry lab for analysis of nitrate, nitrite, phosphate, and silicate concentrations. The samples used in this study were from the depth of approximately 50m to 60m. The nutrients from 60m are compared to GPP at 30m and 60m since the nutrients from 60m and 30m are from the mixed layer so they are homogenized.

Following the cruise, a comprehensive analysis was conducted to establish the relationship between chlorophyll concentrations, current velocity, nutrients concentration and temperature to the dissolved oxygen concentration production. A principal component analysis (PCA) is used to explore the interplay among various factors, including current velocity, nutrient concentrations, chlorophyll concentrations, and water temperature in determining GPP with the assumption that relationship between the

variables is linear. The PCA was done in Python with the help of ChatGPT to find a combination of the factors could explain the variances in GPP.

Results

The oxygen titration of the bottles shows a trend of the bottles from 60m being lower in oxygen production rate compared to 30 m (Table 1 and Figure 4). Oxygen concentrations at 30 m were not statistically significant that those at 60 m (t-test, p = 0.3765).

Table 1. Oxygen Titrations of the bottles. #N/A represent no measurement (unable to open the oxygen bottle)

Latitude	Dark Bottles (uMoles O/kg)		Light Bottles (uMoles O/kg)		Initial (uMoles O/kg)		Incubation (hours)
	60m	30m	60m	30m	60m	30m	
-5	198.79	224.98	211.69	195.19	195.2	197.2	30
-5	214.32	212.94	212.28	203.19			
-5	213.79	202.58	216.27	196.03			
0	223.99	188.24	188.00	189.66	221.1	240.5	15
0	191.67	198.18	185.45	195.68			
0	186.43	187.88	183.95	181.61			
2	194.33	201.01	193.30	204.73	224.2	212.4	29
2	209.03	190.08	192.44	203.80			
2	200.18	#N/A	195.45	201.46			
5	210.31	184.78	190.21	197.50	192.8	207.3	21
5	189.76	189.54	193.49	199.87			
5	188.82	189.34	188.97	208.69			

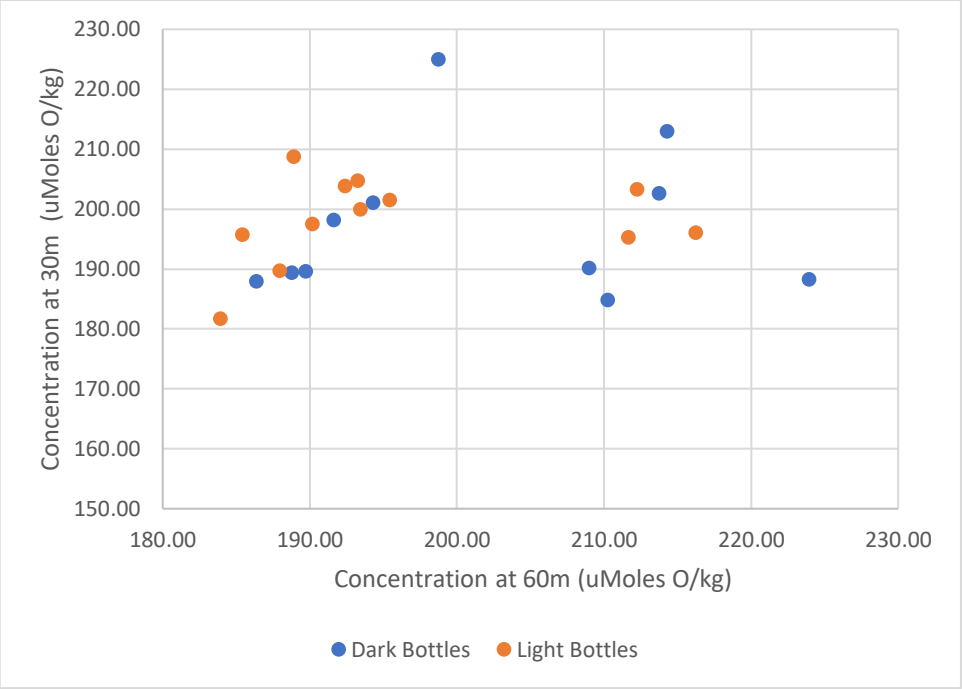

Figure 4. The relationship between the oxygen concentration at 60m and at 30m for the light and dark bottles.

Table 2. The mean respiration rate, mean net photosynthesis, and mean gross photosynthesis for each latitude with their respective standard deviation (Std dev.).

Latitude	Mean Respiration (uMoles O/kg/hr)				Mean Net Photosynthesis (uMoles O/kg/hr)				Mean Gross Photosynthesis (uMoles O/kg/hr)			
	60m	Std Dev.	30m	Std dev.	60m	Std dev.	30m	Std dev.	60m	Std dev.	30m	Std dev.
-5	0.459	0.2939	0.543	0.3737	0.6073	0.0830	0.031	0.1465	1.066	0.3054	0.5747	0.4014
0	-1.358	1.356	-3.272	0.3899	-2.3512	0.1363	-3.435	0.4706	-3.709	1.3633	-6.7067	0.6111
2	-0.792	0.255	3.081	4.9128	-1.0490	0.0535	-0.313	0.0582	-1.841	0.2607	2.7675	4.9131
5	0.166	0.578	-0.924	0.1282	-0.0912	0.1113	-0.251	0.2808	0.075	0.5890	-1.1747	0.3086

The distribution of the mean NPP and mean GPP were plotted across the latitudes (Figure 5). Mean NPP at 30 meters were not statistically significant to those at 60 meters was -0.54 and the p-value is 0.239. The t-test value for mean GPP at 30 meters compared to at 60 meters (t-test, p-value =0.376). The distribution of mean NPP and mean GPP follow the same general trend, where they increase as going away from the equator for both 30 meters and 60 meters (Figure 5). The standard deviation for the

mean GPP at 60 meters and the equator is the largest compared to other points due to an over titration of an oxygen bottle.

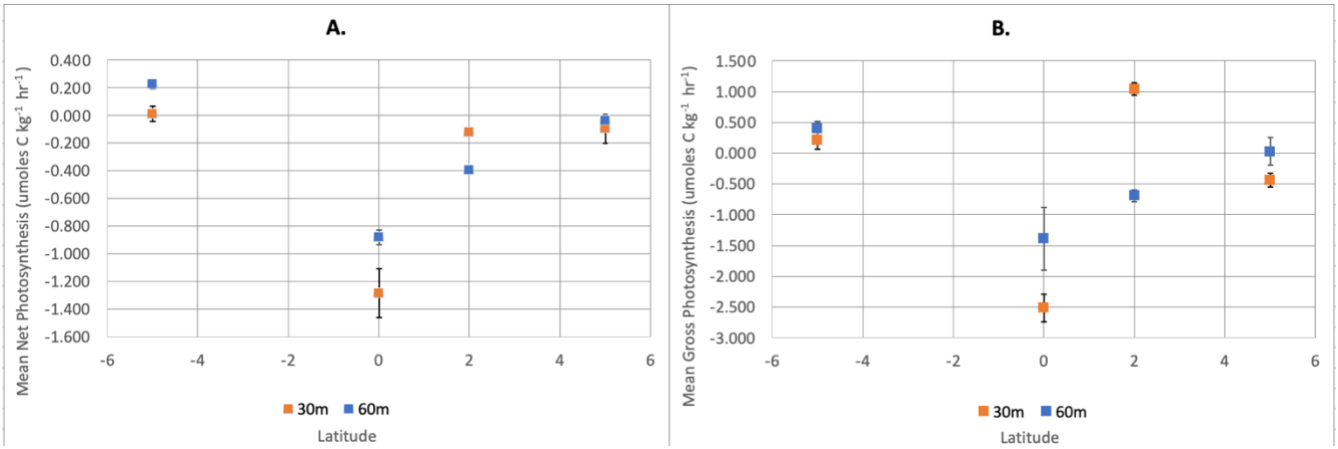

Figure 5. A. Distribution of mean net photosynthesis at depth of 30 and 60 meters from 5º S to 5º N at 167 ºW with error bars showing standard deviation at each latitude for the triplicate measurements. B. Distribution of gross photosynthesis at depth of 30 and 60 meters from 5º S to 5º N at 167º W with error bars showing standard deviation at each latitude for the triplicate measurements.

The distribution of chlorophyll is the highest at the equator for both 30m and 60m (Figure 6A). The further away from equator, the more the chlorophyll fluorescence decreases. The temperature at 2N for 30m and 60m is the same so the point is overlapping each other (Figure 6B). The temperature is the lowest at 2N and highest at 5S.

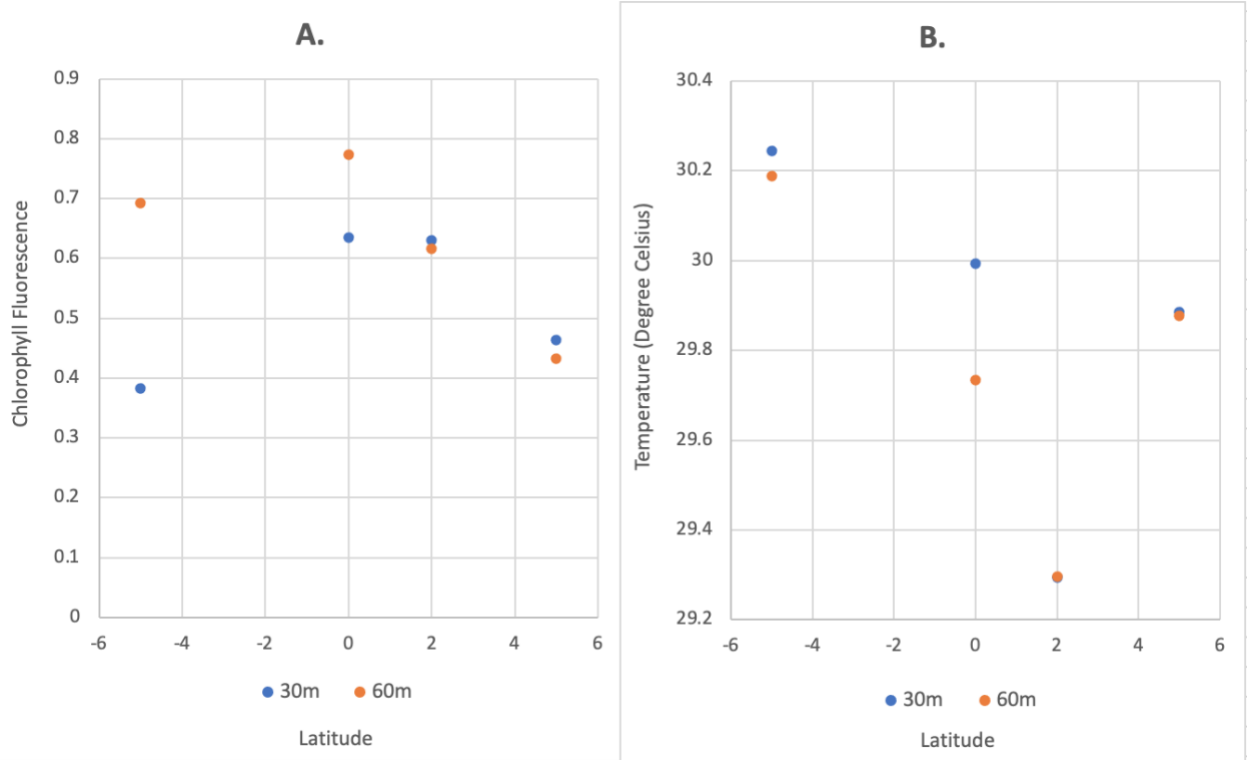

Figure 6. Distribution of A. Chlorophyll Fluorescence and B. Temperature at the depth of 30 and 60 meters from 5º S to 5º N at 167 ºW; measured from the CTD casts.

NO_3 is the highest in concentration at every latitude except for 5N (Figure 7). At 5N, the highest nutrient concentration is $Si(OH)_4$. $Si(OH)_4$ increases from 5S to 5N while NO3 increases till 5N, where the concentration decrease significantly in comparison to the other nutrients. From 5S to 2N, the NH_4 was the lowest nutrient concentration. At 5N, the lowest nutrient concentration was NO_2.

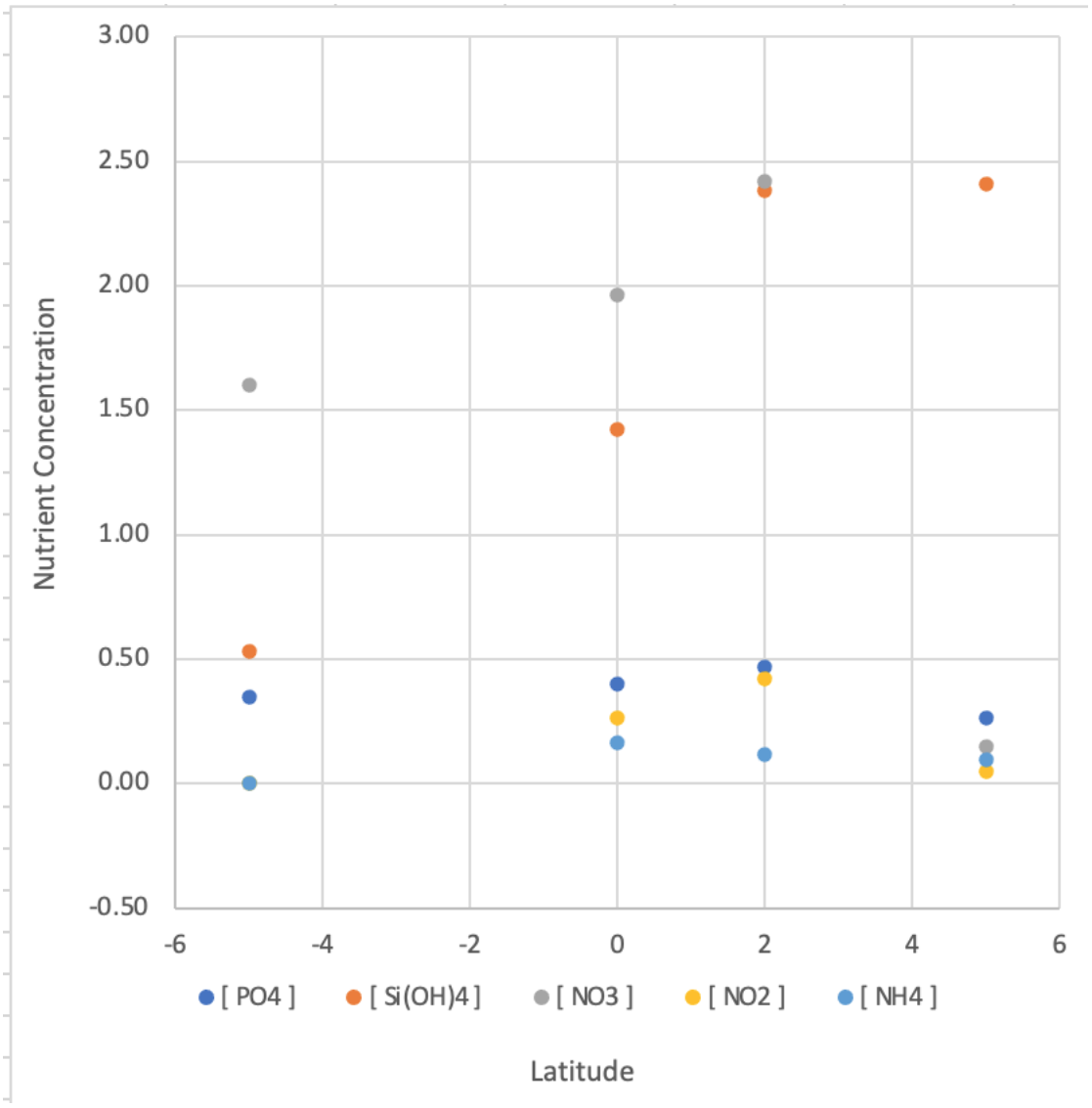

Figure 7. The distribution of nutrients concentration, PO4, Si(OH)4, NO3, NO2, and NH4 at the depth of approximately 50 meters to 60 meters from 5º S to 5º N at 167 ºW.

The zonal velocity was the strongest at 2º N and 5º N at the depth of 30 meters where, 2º N is going westward and 5º N is going eastward (Figure 8). The zonal velocity at the equator for 30 meters is also going westward at -0.5 m/s. At 5º S and 30 meters, the velocity is westward at -0.4 m/s. At 60 meters of depth, the zonal velocity for 2º N decreases by 0.4 m/s and for 5º N, it increases to 0.1 m/s. At the equator and 5º S for

60 meters, the strength and direction of the current stay the same as in 30 meters of depth.

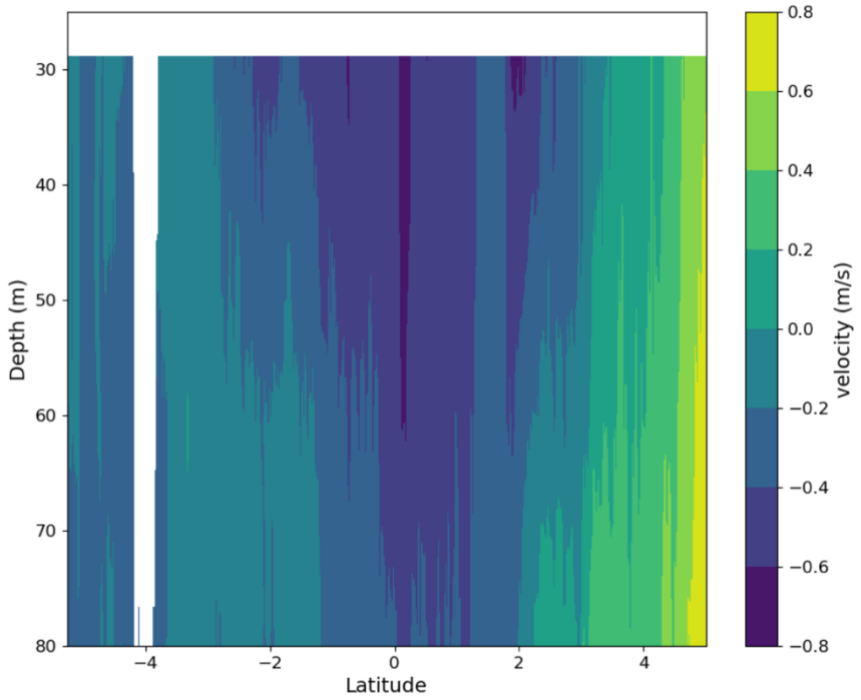

Figure 8. The zonal velocity (m/s) from 25 to 80 meters of depth across 5º S to 5º N at 167º W. East-west direction, where negative velocity is in the westward direction and positive velocity is in the eastward direction.

The zonal velocity was plotted against the mean NPP for each latitude at the depth of 30 meters and 60 meters (Figure 9 and 10). There was a significant relationship observed between NPP and zonal current velocity (Pearson test, R^2 = 0.437, p-value = 0.0371). No significant relationship was observed between GPP and zonal current velocity (Pearson test, R^2 = 0.361, p-value = 0.0904).

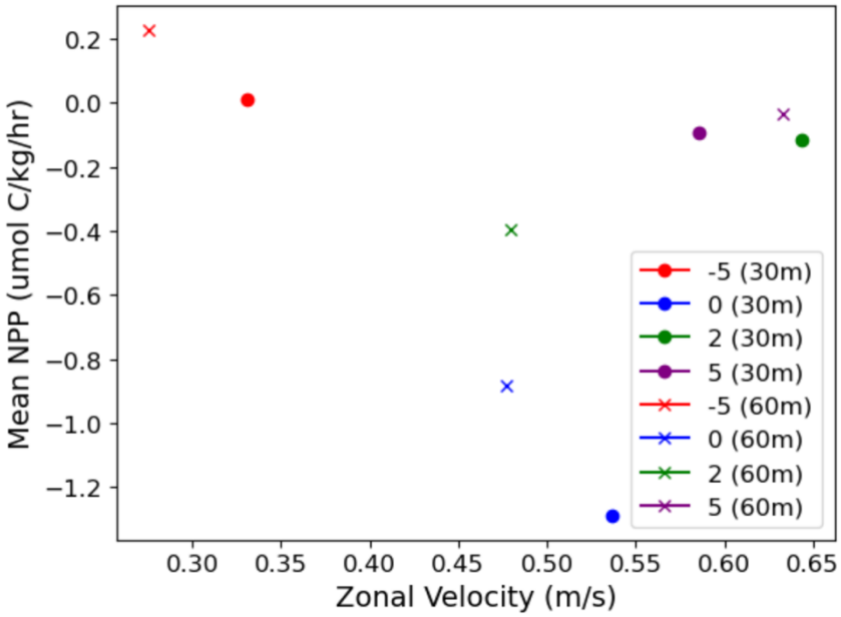

Figure 9. Zonal velocity compared to the mean NPP for latitude -5, equator, 2, and 5 at 30m and 60m of depth.

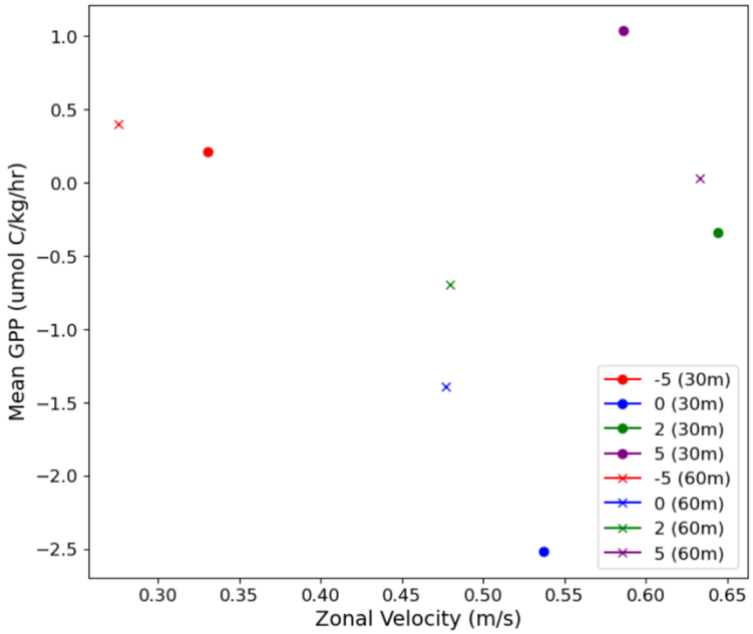

Figure 10. Zonal velocity compared to the GPP for latitude -5, equator, 2, and 5 at 30m and 60m of depth.

At the depth of 30 meters and 60 meters, the depths were within the mixed layered for all of the stations. Due to this, the dissolved nutrients within the mixed layered would not have a lot of variations and be consistent throughout the layer. The Mean GPP plotted is from the depth of 60 meters compared to the nutrients concentration of PO_4, $Si(OH)_4$, NO_3, NO_2, and NH_4 (Figure 11). No statistical significant relationships were observed between GPP and nutrient concentrations (Pearson correlation test, p-value > 0.1).

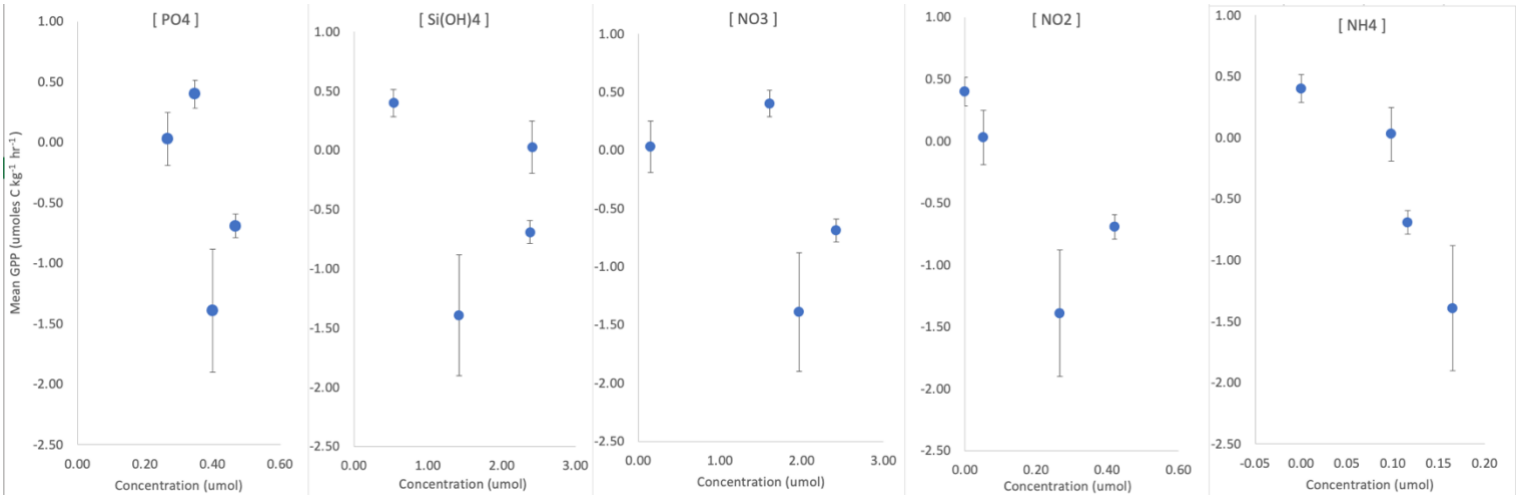

Figure 11. Dissolved Nutrients, PO_4, $Si(OH)_4$, NO_3, NO_2, and NH_4, concentrations in umol compared to the mean GPP within the mixed layer at 60 meters of depth.

The fluorescence was plotted against the mean GPP for the depth 30m and 60m. No statistically significant correlation was found between GPP and chlorophyll fluorescence (Pearson correlation test, p-value of 0.375 > 0.1).

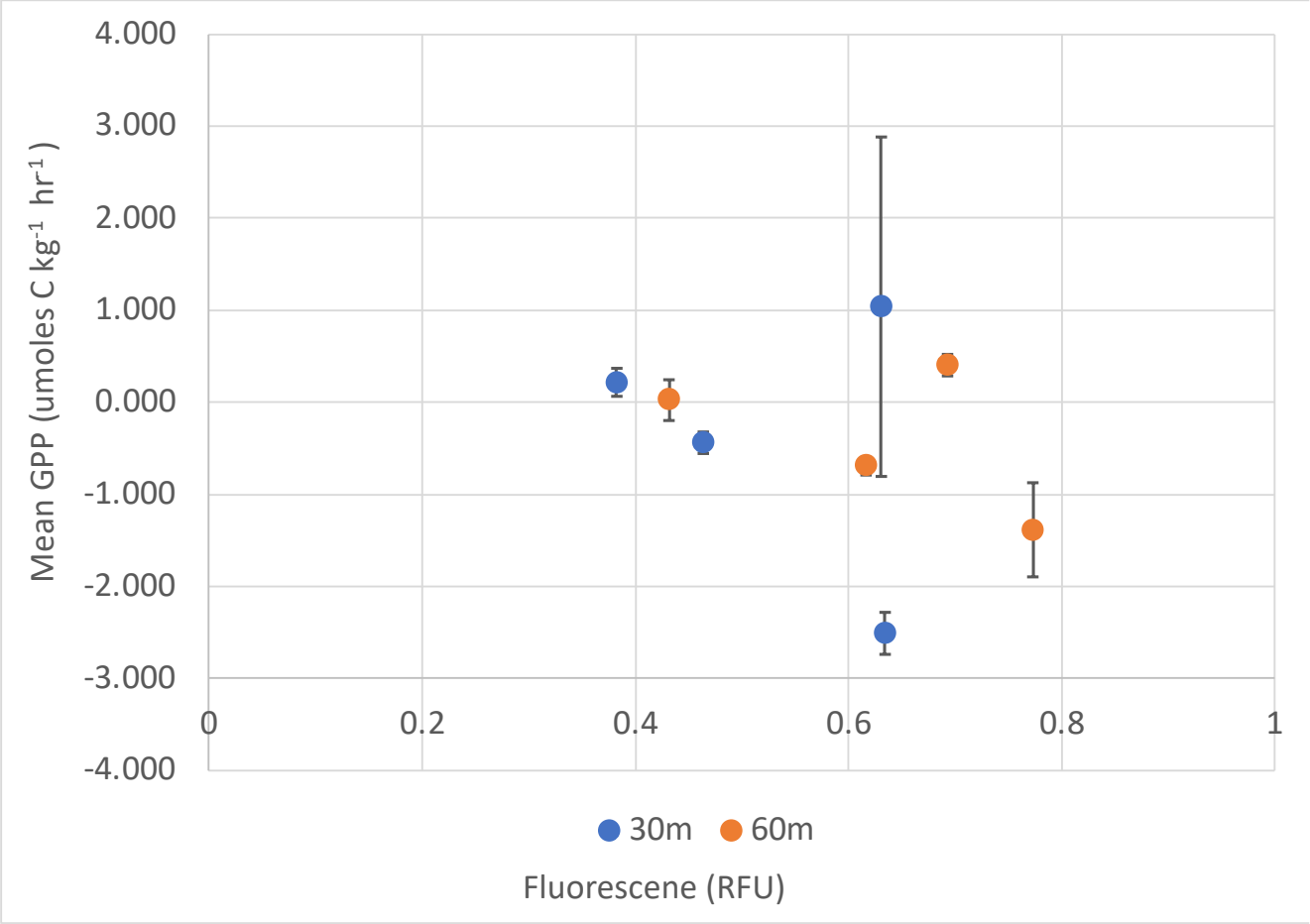

Figure 12. The fluorescence compared to the mean GPP at 30m and 60m. Fluorescence is also representing the chlorophyll concentration.

The temperature was measured from the CTD and plotted against the mean GPP at 30 meters and 60 meters. No statistically significant correlation was found between GPP and temperature (Pearson correlation test, p-value of 0.269 > 0.1) (Figure 13).

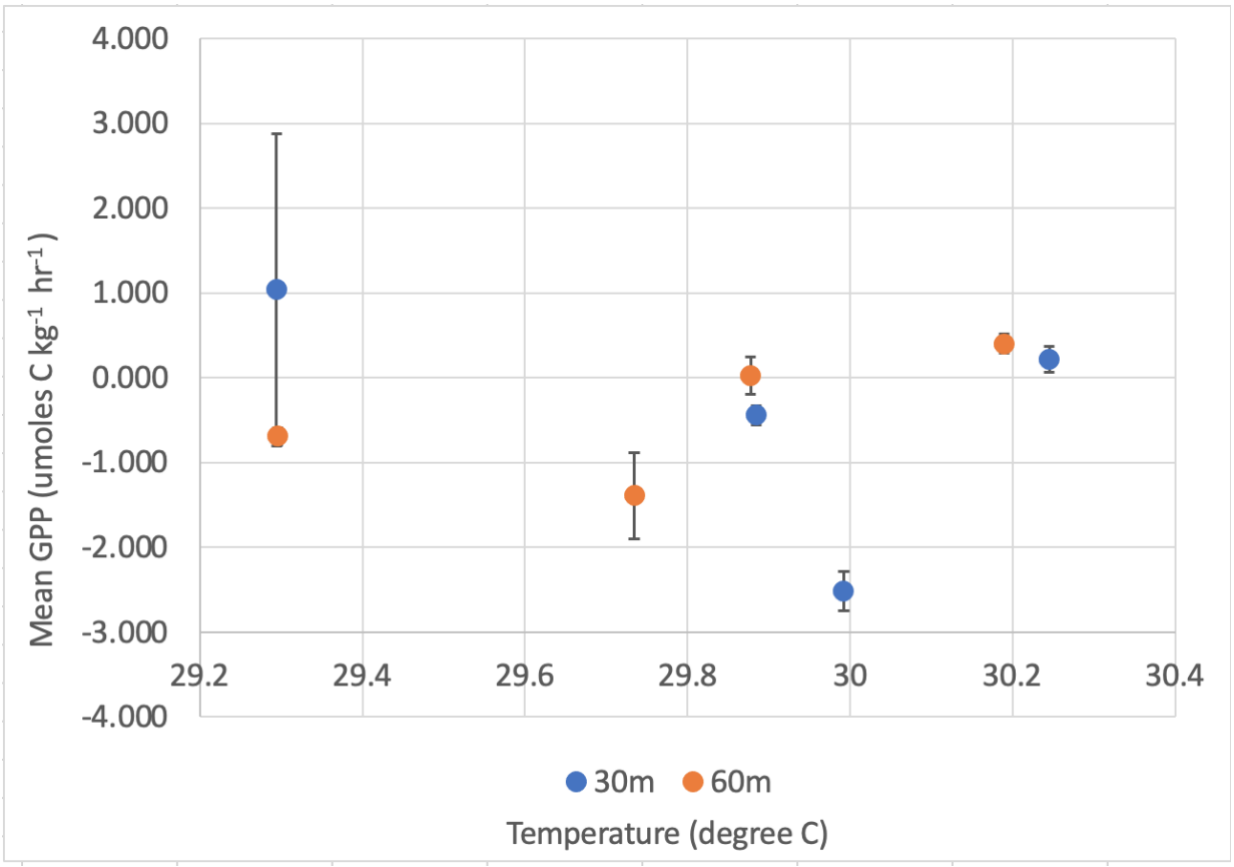

Figure 13. Temperature in Celsius compared to the Mean GPP at depths of 30m and 60m.

The principal component 1 explains 54.18% of the variance and principal component 2 explains 29.73% of the variances for GPP at 30 meters when considering the independent factors; temperature, PO_4, $Si(OH)_4$, NO_2, NO_3, NH_4), zonal velocity and chlorophyll (Chl) (Figure 12).

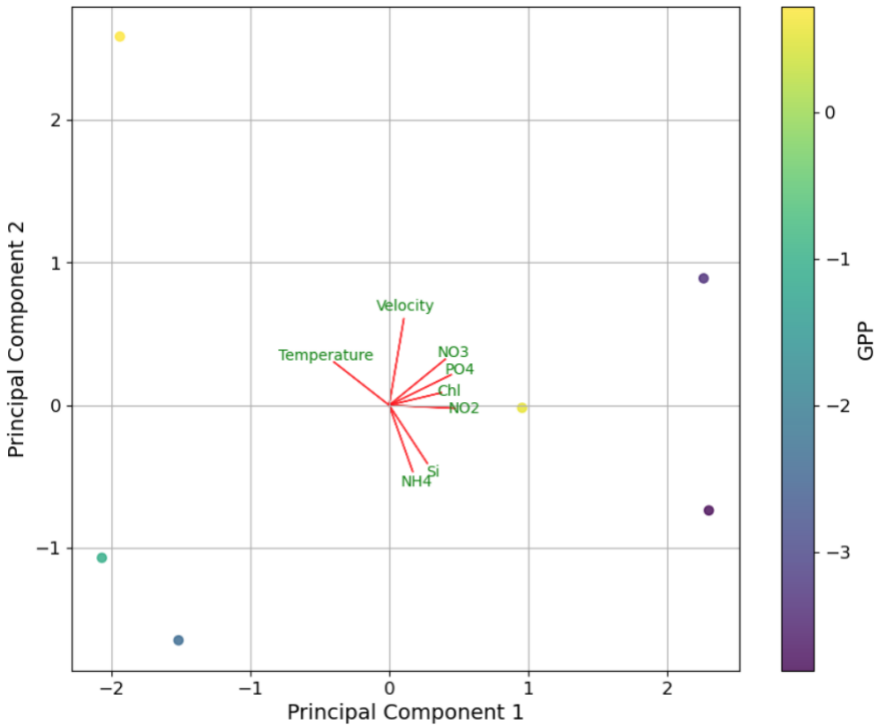

Figure 14. Comparison of Component 1 and 2 with GPP at 30 and 60 meters with the independent variables including temperature, dissolved nutrients (PO_4, $Si(OH)_4$, NO_2, NO_3, NH_4), zonal velocity and Chlorophyll (Chl).

Discussion

In this study, I measured and calculated the GPP in addition to NPP compared to satellite data that only measure NPP, which doesn't account for the respiration. Based on previous studies, the expected average NPP in the western equatorial Pacific was 5.9 ± 0.9 mmol O_2 m^{-2} d^{-1} and the expected average GPP was 21 ± 34 mmol O_2 m^{-2} d^{-1} (Stanley et al., 2010). The mean NPP in this study ranged from −83.94 to 94.862 mmol O_2 m^{-2} d^{-1} (-3.435 to 0.6073 umol O_2 kg^{-1} hr^{-1}) (Table 2). This range is much bigger than the expect average NPP. The mean GPP in this study ranged from −163.82 to 26.05 mmol O_2 m^{-2} d^{-1} (-6.7067 to 1.066 umol O_2 kg^{-1} hr^{-1}) (Table 2). The upper

range of mean GPP is within the range of the expected average GPP but the lower range is outside of the expected.

In this study, some of the primary productivity values were negative (Figure 5). A negative primary productivity value means that the respiration rate exceeds the photosynthesis rate. This can occur when the ecosystem is under stress conditions, such as high temperature. In high temperature, the biomass of phytoplankton may decrease or change in community composition which result an impact on the amount of photosynthesis done by the primary producers (Arteaga & Rousseaux, 2023). The lowest primary productivity value was at the equator, but the highest temperature was at 5S (Figure 5, Figure 6B). Since I was not able to directly measure the NPP rate, this may have been a result due to my method. The phytoplankton may have not responded well to the incubation experiment, since the incubations was under twenty-four hours compared the standard 5 days incubation for biochemical oxygen demand (Willhelm, 2009). Another reason for the high respiration rate may be due to the presence of bacteria. The water collected were not filtered so there are organisms in the incubated bottles. During the incubation of longer than 15 hours, the bacteria could increase their respiration rate (Garcia-Robledo et al., 2016). The increase in respiration rate could be the reason why some of the primary productivity values were negative.

The pattern of the NPP and GPP rates is the inverse of the chlorophyll pattern, where chlorophyll is highest at the equator and decrease the further away from the equator. This was difference from what was expected. Previous studies show that the change in NPP has a linear relationship with the change in chlorophyll (Marpaung et al.,

2022). However, in this study, there is an inverse relationship between NPP and chlorophyll. This suggest that chlorophyll is not a good indicate of NPP in this region.

The nutrient pattern was unexpected compared to previous studies. In previous studies, the nutrients are at the highest concentration at the equator and decreasing going northward and southward (Wyrtki & Kilonsky, 1984). The nutrients in this study were highest at 2N and then decrease going north and south of 2N (Figure 7). It is expected that the nutrients would be highest at the equator due to the upwelling occurring at the equator (Wyrtki & Kilonsky, 1984). It was observed that the zonal velocity was the highest at the equator which indicate that upwelling would be greater at the equator (Figure 8). However, a greater upwelling would lead to higher nutrient concentration which was not observed.

The NPP and GPP does not seem to be correlated with the zonal velocity, dissolved nutrients, chlorophyll, and temperature. However, a combination of these factors can explain for about 54.18% of the variance in GPP (Figure 12). There is a missing 46.82% that is not factored for in the variance of GPP. Temperature being a large factor since the temperature in this region was higher and had a smaller range in temperature. Temperature was also the only factor that had a negative relationship with GPP. The high temperature may have led to metabolic rate slowing down after passing a certain threshold. Previous studies have shown that rising temperatures negatively impact NPP and increase the respiration rate (Krumhardt et al., 2017). Warmer water tends to have smaller phytoplankton, which exhibit lower NPP rates . As discussed before GPP is the combination of NPP and respiration (equation 1c), since NPP is

decreasing and respiration is increasing, the GPP would decrease. Respiration would decrease since the process decreases the amount of oxygen.

Limiting factors are the few sampling sites. I ran out of oxygen bottles to collect water samples in between the stations and did not have enough time to titrate the bottles between stations. When redoing this project, I would plan to have more oxygen bottles to collect the water samples from more stations to have more data points. I would also plan to look at satellite derived NPP data on the area of study for a comparison of accuracy.

Conclusion

In conclusion, this study highlights the multiple factors that affect the GPP in the western equatorial Pacific. The principal component analysis showed that temperature and NO_2 were the most corresponding variable with GPP. Temperature had a negative relationship with GPP while NO_2 had a positive relationship with GPP. The PCA showed the principal component accounted for 54.18% of the variance in GPP. This finding contributes to our understanding of NPP and GPP in this region, to address the gap. The implication of this research is significant considering the impact of climate change. Further research is needed to explore the missing 46.82% not accounted for by looking at additional factors to have a more comprehensive understanding of the GPP in the western equatorial Pacific.

Acknowledgement

I would like to thank advisor, Francois Ribalet, for his continuous support through this project and OCEAN 445 professors, who helped on the ship and with this project. I would like to thank the crew and captain of the Thomas G. Thompson for their support throughout the cruise and helping me collect the samples. I would also like to thank my classmates of OCEAN'24 for helping me collect the samples and Cody Cruz for processing the ADCP data. Thank you to the School of Oceanography at the University of Washington for funding this wonderful opportunity.

References

Arteaga, L. A., & Rousseaux, C. S. (2023). Impact of Pacific Ocean heatwaves on phytoplankton community composition. *Communications Biology*, *6*. https://doi.org/10.1038/s42003-023-04645-0

Behrenfeld, M. J., & Falkowski, P. G. (1997). Photosynthetic rates derived from satellite-based chlorophyll concentration. *Limnology and Oceanography*, *42*(1), 1–20. https://doi.org/10.4319/lo.1997.42.1.0001

Behrenfeld, M. J., Worthington, K., Sherrell, R. M., Chavez, F. P., Strutton, P., McPhaden, M., & Shea, D. M. (2006). *Controls on tropical Pacific Ocean productivity revealed through nutrient stress diagnostics* | *Nature*. https://www.nature.com/articles/nature05083

Coale, K. H., Johnson, K. S., Fitzwater, S. E., Gordon, R. M., Tanner, S., Chavez, F. P., Ferioli, L., Sakamoto, C., Rogers, P., Millero, F., Steinberg, P., Nightingale, P., Cooper, D., Cochlan, W. P., Landry, M. R., Constantinou, J., Rollwagen, G., Trasvina, A., & Kudela, R. (1996). A massive phytoplankton bloom induced by an ecosystem-scale iron fertilization experiment in the equatorial Pacific Ocean. *Nature*, *383*(6600), 495–501. https://doi.org/10.1038/383495a0

D'Alelio, D., Rampone, S., Cusano, L. M., Morfino, V., Russo, L., Sanseverino, N., Cloern, J. E., & Lomas, M. W. (2020). Machine learning identifies a strong association between warming and reduced primary productivity in an oligotrophic ocean gyre. *Scientific Reports*, *10*(1), Article 1. https://doi.org/10.1038/s41598-020-59989-y

Feng, J., Li, D., Zhang, J., & Zhao, L. (2022). Variations and Environmental Controls of Primary Productivity in the Amundsen Sea. *Frontiers in Marine Science*, *9*. https://www.frontiersin.org/articles/10.3389/fmars.2022.891663

Field, C. B., Behrenfeld, M. J., Randerson, J. T., & Falkowski, P. (1998). Primary Production of the Biosphere: Integrating Terrestrial and Oceanic Components. *Science*, *281*(5374), 237–240. https://doi.org/10.1126/science.281.5374.237

Fine, R., Lukas, R., Bingham, F., Warner, M., & Gammon, R. (1994). The Western Equatorial Pacific—A water mass crossroads. *Journal of Geophysical Research*, *99*, 25063–25080. https://doi.org/10.1029/94JC02277

Firing, E., Hummon, J., & Chereskin, T. (2012). Improving the Quality and Accessibility of Current Profile Measurements in the Southern Ocean. *Oceanography*, *25*(3), 164–165. https://doi.org/10.5670/oceanog.2012.91

Garcia-Robledo, E., Borisov, S., Klimant, I., & Revsbech, N. P. (2016). Determination of Respiration Rates in Water with Sub-Micromolar Oxygen Concentrations. *Frontiers in Marine Science*, *3*. https://doi.org/10.3389/fmars.2016.00244

Hidaka, K. (1972). Physical oceanography of upwelling. *Geoforum*, *3*(3), 9–21. https://doi.org/10.1016/0016-7185(72)90082-6

Huston, M. A., & Wolverton, S. (2009). The global distribution of net primary production: Resolving the paradox. *Ecological Monographs*, *79*(3), 343–377. https://doi.org/10.1890/08-0588.1

Krumhardt, K. M., Lovenduski, N. S., Long, M. C., & Lindsay, K. (2017). Avoidable impacts of ocean warming on marine primary production: Insights from the

CESM ensembles. *Global Biogeochemical Cycles*, *31*(1), 114–133. https://doi.org/10.1002/2016GB005528

Krumhardt, K. M., Lovenduski, N. S., Long, M. C., Luo, J. Y., Lindsay, K., Yeager, S., & Harrison, C. (2020). Potential Predictability of Net Primary Production in the Ocean. *Global Biogeochemical Cycles*, *34*(6), e2020GB006531. https://doi.org/10.1029/2020GB006531

Labasque, T., Chaumery, C., Aminot, A., & Kergoat, G. (2004). Spectrophotometric Winkler determination of dissolved oxygen: Re-examination of critical factors and reliability. *Marine Chemistry*, *88*(1), 53–60. https://doi.org/10.1016/j.marchem.2004.03.004

Longhurst, A., Sathyendranath, S., Platt, T., & Caverhill, C. (1995). An estimate of global primary production in the ocean from satellite radiometer data. *Journal of Plankton Research*, *17*(6), 1245–1271. https://doi.org/10.1093/plankt/17.6.1245

Lotze, H. K., Tittensor, D. P., Bryndum-Buchholz, A., Eddy, T. D., Cheung, W. W. L., Galbraith, E. D., Barange, M., Barrier, N., Bianchi, D., Blanchard, J. L., Bopp, L., Büchner, M., Bulman, C. M., Carozza, D. A., Christensen, V., Coll, M., Dunne, J. P., Fulton, E. A., Jennings, S., … Worm, B. (2019). Global ensemble projections reveal trophic amplification of ocean biomass declines with climate change. *Proceedings of the National Academy of Sciences*, *116*(26), 12907–12912. https://doi.org/10.1073/pnas.1900194116

Lukas, R., & Lindstrom, E. (1991). The mixed layer of the western equatorial Pacific Ocean. *Journal of Geophysical Research: Oceans*, *96*(S01), 3343–3357. https://doi.org/10.1029/90JC01951

Mackey, D. J., Parslow, J., Higgins, H. W., Griffiths, F. B., & O'Sullivan, J. E. (1995). Plankton productivity and biomass in the western equatorial Pacific: Biological and physical controls. *Deep Sea Research Part II: Topical Studies in Oceanography*, *42*(2–3), 499–533. https://doi.org/10.1016/0967-0645(95)00038-R

Marpaung, S., Prayogo, T., Yati, E., Purwanto, A. D., Nandika, M. R., Domiri, D. D., & Kushardono, D. (2022). ANALISIS KARAKTERISTIK NET PRIMARY PRODUCTIVITY DAN KLOROFIL-A DI LAUT BANDA DAN SEKITARNYA. *Jurnal Ilmu dan Teknologi Kelautan Tropis*, *14*(1), Article 1. https://doi.org/10.29244/jitkt.v14i1.36757

Moore, J. K., Fu, W., Primeau, F., Britten, G. L., Lindsay, K., Long, M., Doney, S. C., Mahowald, N., Hoffman, F., & Randerson, J. T. (2018). Sustained climate warming drives declining marine biological productivity. *Science*, *359*(6380), 1139–1143. https://doi.org/10.1126/science.aao6379

Mountford, K. (1969). Measuring Dissolved Oxygen as an Indicator of Primary Productivity. *Chesapeake Science*, *10*(3/4), 327–330. https://doi.org/10.2307/1350478

Sigman, D., & Hain, M. (2012). The Biological Productivity of the Ocean. *Nature Education*, *3*, 1–16.

Silsbe, G. M., Behrenfeld, M. J., Halsey, K. H., Milligan, A. J., & Westberry, T. K. (2016). The CAFE model: A net production model for global ocean phytoplankton. *Global Biogeochemical Cycles*, *30*(12), 1756–1777. https://doi.org/10.1002/2016GB005521

Stanley, R. H. R., Kirkpatrick, J. B., Cassar, N., Barnett, B. A., & Bender, M. L. (2010). Net community production and gross primary production rates in the western equatorial Pacific. *Global Biogeochemical Cycles*, *24*(4). https://doi.org/10.1029/2009GB003651

Stock, C. A., John, J. G., Rykaczewski, R. R., Asch, R. G., Cheung, W. W. L., Dunne, J. P., Friedland, K. D., Lam, V. W. Y., Sarmiento, J. L., & Watson, R. A. (2017). Reconciling fisheries catch and ocean productivity. *Proceedings of the National Academy of Sciences*, *114*(8), E1441–E1449. https://doi.org/10.1073/pnas.1610238114

Tagliabue, A., Kwiatkowski, L., Bopp, L., Butenschön, M., Cheung, W., Lengaigne, M., & Vialard, J. (2021). Persistent Uncertainties in Ocean Net Primary Production Climate Change Projections at Regional Scales Raise Challenges for Assessing Impacts on Ecosystem Services. *Frontiers in Climate*, *3*. https://www.frontiersin.org/articles/10.3389/fclim.2021.738224

Venables, H., & Moore, C. M. (2010). Phytoplankton and light limitation in the Southern Ocean: Learning from high-nutrient, high-chlorophyll areas. *Journal of Geophysical Research: Oceans*, *115*(C2). https://doi.org/10.1029/2009JC005361

Villacieros-Robineau, N., Gilcoto, M., Pardo, P. C., & Barton, E. D. (2021). Wave Regime and Wave-Current Coupling in an Upwelling–Driven Bay: Seasonal and Inter-Annual Variability. *Journal of Geophysical Research: Oceans*, *126*(11), e2021JC017540. https://doi.org/10.1029/2021JC017540

Wang, Y., Wang, K., Bai, Y., Wu, D., & Zheng, H. (2023). Research progress in calculating net community production of marine ecosystem by remote sensing.

Frontiers in Marine Science, *10*. https://www.frontiersin.org/articles/10.3389/fmars.2023.1191013

Willhelm, F. M. (2009). *Pollution of Aquatic Ecosystems I - ScienceDirect*. https://www.sciencedirect.com/science/article/pii/B9780123706263002222

Winckler, G., Anderson, R. F., Jaccard, S. L., & Marcantonio, F. (2016). Ocean dynamics, not dust, have controlled equatorial Pacific productivity over the past 500,000 years. *Proceedings of the National Academy of Sciences*, *113*(22), 6119–6124. https://doi.org/10.1073/pnas.1600616113

Wyrtki, K., & Kilonsky, B. (Directors). (1984, February 1). *Mean Water and Current Structure during the Hawaii-to-Tahiti Shuttle Experiment in: Journal of Physical Oceanography Volume 14 Issue 2 (1984)*. https://journals.ametsoc.org/view/journals/phoc/14/2/1520-0485_1984_014_0242_mwacsd_2_0_co_2.xml